

Micromechanical performance of interfacial transition zone in fiber-reinforced cement matrix

V Zacharda¹, J Němeček¹ and P Štemberk¹

¹ Czech Technical University, Thákurova 7, 166 29 Prague 6, Czech Republic

E-mail: vojtech.zacharda@fsv.cvut.cz

Abstract. The paper investigates microstructure, chemical composition and micromechanical behavior of an interfacial transition zone (ITZ) in steel fiber reinforced cement matrix. For this goal, a combination of scanning electron microscopy (SEM), nanoindentation and elastic homogenization theory are used. The investigated sample of cement paste with dispersed reinforcement consists of cement CEM I 42,5R and a steel fiber TriTreg 50 mm. The microscopy revealed smaller portion of clinkers and larger porosity in the ITZ. Nanoindentation delivered decreased elastic modulus in comparison with cement bulk (67%) and the width of ITZ ($\sim 40 \mu\text{m}$). The measured properties served as input parameters for a simple two-scale model for elastic properties of the composite. Although, no major influence of ITZ properties on the composite elastic behavior was found, the findings about the ITZ reduced properties and its size can serve as input to other microstructural fracture based models.

1. Introduction and motivation

Nowadays, the fiber reinforced concrete (FC) is a popular building material which is increasingly utilized for structural elements. Fiber concrete is characterized with randomly dispersed fibers that may have different length, thickness, composition and shape. The fibers are made from a wide range of materials like glass, steel, carbon or different kinds of synthetic materials. The most frequent material used for structural purposes is steel due to its beneficial role in enhancing composite tensile strength properties, permeability or impact resistance. For a good mechanical performance of FC the distribution and orientation of fibers in the composite volume plays a critical role.

The macroscopic FC composite behavior is also directly influenced by micromechanics of a fiber and interfacial zone that surrounds it. In the last decade, a lot of research on micromechanical characteristics of cementitious composite material has been conducted. With the development of advanced experimental techniques, like e.g. nanoindentors or scanning electron microscopes, it was possible to determine a variety of microscale material properties for cement paste [1,2,14], concrete [3], UHPC [4], mortars [5] and other materials. Microlevel elastic and viscoelastic properties, chemical composition or the microstructure of interfacial transition zone (ITZ) [3,5,6,7] have been revealed. So far, little research has been carried out for micromechanical properties of ITZ which is known for different morphology and chemical composition compared to the bulk cementitious matrix. Therefore investigations carried out in this paper are focused on micromechanics of a fiber and its influence on the overall composite behavior from the mechanical point of view.



Concrete is generally taken as a multiscale material consisting of several phases. At least two phases – aggregate and cement paste must be considered. But more correctly concrete is composed of at least three phases – aggregate, cement paste and interfacial transition zone that forms a thin layer surrounding the aggregate with different chemical and mechanical properties. If fibers are used in the concrete mixture they act as a separate phase surrounded by an additional ITZ with different mechanical properties [8,9,10,11] and microstructure [5,6,7] compared to the bulk matrix. In general, ITZ is located around each inclusion (sand, aggregate, steel fiber, reinforcement) in the concrete and the varying properties are caused by different reasons like locally different water/cement ratio, different confinement or compaction, different boundary conditions, etc.

Local differences of morphology and chemical composition can be sensed by microscopy whereas local mechanical differences can be well measured using nanoindentation. Nanoindentation has been already successfully used for characterization of a bulk cementitious matrix, The ITZ around aggregate [12] or reinforcement [8,9] or steel fiber in reinforcement in mortar [10], or various cementitious mixtures [12]. Again, the research conducted in this paper concentrates on ITZ around fibers in a normal FC (Fig. 1) and aims to quantify its local and overall influence on mechanical performance of the composite.



Figure 1. Tension fracture of a beam with pulled out fibers

2. Fiber concrete and the role of ITZ

2.1. Macroscopic mechanical role of fibers

The concrete with dispersed fiber reinforcement delivers the composite improved material characteristics and properties like higher ductility, toughness, tensile strength and impact resistance. Fibers can reduce shrinkage of material creep and reduce localized cracking by local bridging mechanism. Since the direction of a mechanical load may vary it is critically important to distribute homogeneously the fibers with fibers randomly oriented within the mixture or a cast element. Unfortunately, an addition of fibers increases mixture viscosity in a fresh state and makes mixing more difficult and energy expensive. Thus, lower volume ratios in the order of a few percent can be effectively used in reality.

The mechanical role of a fiber lies in bridging the cracks and transferring locally high tensile stresses that would otherwise lead to concrete cracking, to other composite locations. This leads to more spread or distributive fracture that is macroscopically manifested as increased ductility and the composite exhibits larger number of smaller cracks. Depending on a fiber-matrix bond, the deformation mechanism of a fiber involves either pulling out of fiber from the matrix or (less frequently) fiber rupture.

2.2. Microstructural effects of a fiber

As stated earlier, fiber is surrounded by ITZ zone which is chemically and mechanically different for the bulk. The scale of ITZ is in the order of tens of micrometres which is also a scale of hydration products within the cement matrix. There are five main hydration products in the hardened matrix, namely the calcium-silica or calcium-alumina hydrates (C-S-H and C-A-H gel), Portlandite (CH), unhydrated clinkers and pores.

Microstructure of ITZ around fibers is characterized with less portion of clinkers and more C-S-H gel and CH than in the bulk matrix. Microscopic studies show that ITZ zone contains smaller clinker or CH grains, has a higher local water/cement ratio, and thus a higher porosity [6,7]. It causes a weaker bond of the matrix to the fiber surface. The influence of the rigid obstacle formed by a fiber in the matrix is sometimes called the wall effect [7]. From the micromechanical point of view, the main difference between ITZ and the cement matrix bulk is still in the porosity which reduces the modulus of elasticity of ITZ by tens of percent. The thickness of ITZ is irregular and is related to the width of the fiber [12].

Micromechanical studies show that the average modulus of elasticity measured by nanoindentation for clinker is about ~ 120 GPa, low density C-S-H gel ~ 20 GPa, high density C-S-H gel ~ 31 GPa and CH ~ 40 GPa [13;14]. In the paper by Zhu and Bartos [9], different ITZ properties are found also for the bottom and top sides of the horizontal steel bar in cement. For instance, at the distance of 10 – 30 µm below the steel bar, the interfacial *E* modulus and hardness bottom side the steel bar was only 56% and 70% of the bulk, respectively [8]. The paper Hashin – Monteiro [11] says that the modulus of elasticity can be reduced in the ITZ to about 50% of its normal value so the ITZ is the weak link in concrete.

3. Material and microstructure

3.1. Tested material and sample preparation

The micromechanical performance of a fiber in cementitious matrix was studied on a sample of cement paste with a single embedded steel fiber. Cement paste was made from cement CEM I 42,5R with water to cement ratio equal to 0,4. As a reinforcement a straight steel fiber with Z-anchors (brand name TriTreg, Trinec, CZ) with length of 50 mm and thickness of 1,05 mm was used. The sample had a cylindrical shape with height of 65 mm and diameter of 30 mm. It was unmoulded three days after casting and stored in water for 28 days. After hardening, the samples were cut into slices (disks), the surface grinded and polished by a metallographic procedure [1] and prepared for testing by nanoindentation.

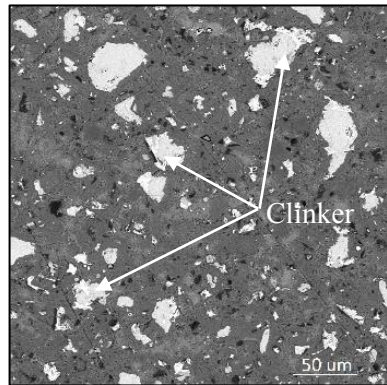
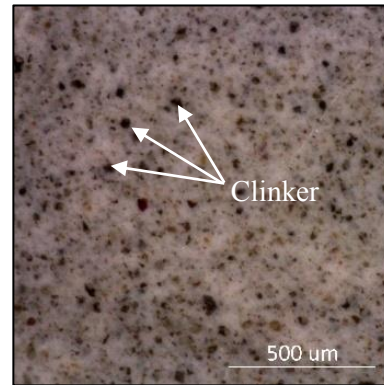
3.2. Characteristics of a cement matrix

Scanning electron microscopy and optical microscopy were employed for microstructural and chemical analysis of the matrix. Nanoindentation has been employed for characterization of individual hydration components of the matrix. The work has been conducted by the authors elsewhere [1] and only major conclusions are summarized here. Based on SEM imaging (12 images covering matrix area of 300 x 300 µm) and image analysis volume fractions have been assessed, Tab. 1.

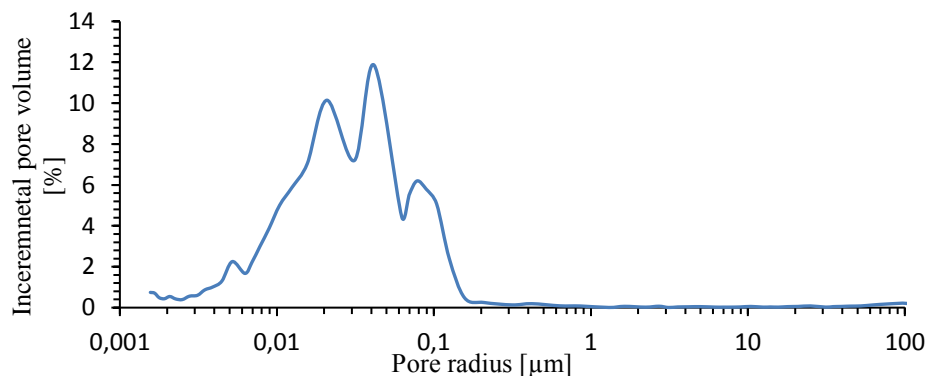
Table 1. Volume ratio of single phases in cement CEM I 42,5R from SEM

Phase	C-S-H gel	CH	C-A-H	Clinker	Pores and cracks
Volume ratio [%]	67,69	17,46	5,54	9,01	0,29

As a complementary measurement, optical microscopy was performed using a digital camera (DinoCapture). The optical photo illustrates distribution of the observable phases in real colours (Fig. 3). The black and dark coloured spots in Fig. 3 belong to clinkers whereas lighter colours stand for main hydration products (C-S-H and CH). Capillary and smaller porosity cannot be revealed in the resolution of the optical picture.

**Figure 2.** SEM photo of cement matrix**Figure 3.** Optical microscopy

More precise porosity measurement was performed by mercury intrusion porosimetry (MIP) which gives overall porosity as well as pore distribution. A dried sample crushed from a larger piece with millimetre dimensions has been used for the analysis. The MIP technique gives pore sizes in about 0.001-100 µm. Figure 4 shows the distribution curve of pores in the tested sample.

**Figure 4.** Distribution of pores

3.3. Microscopy of ITZ around fibers

Scanning electron microscopy was applied to show different distribution of phases in the microstructure. Six SEM photos were taken at random positions around the fiber. The scans cannot show all phases in the same contrast. The steel fiber with the highest atomic ratio is indicated by white colour whereas other phases are in dark grey colours. Unhydrous clinker particles can be detected as the lightest grey particles in the hydrated matrix (Fig. 5). The ITZ zone is characterized with less portion of the clinkers as a consequence of a locally higher water to cement ratio and more pronounced hydration of these phases. In contrast, higher w/c ratio causes increased porosity in the ITZ which can also be revealed from the images. Based on the different morphology, porosity and phase distribution an approximate width of ITZ is depicted in Fig. 6.

The chemical composition of ITZ was investigated by energy dispersive spectrometer. Output from EDS line scans made in perpendicular directions to the fiber are depicted in Fig. 7. Relative concentrations of the five main elements are shown in Fig. 7 as their relative weight ratios. Approximately equal elemental composition (with local fluctuations caused mainly by clinker inclusions) has been found which does not indicate any preferential or altered hydration in ITZ compared to bulk.

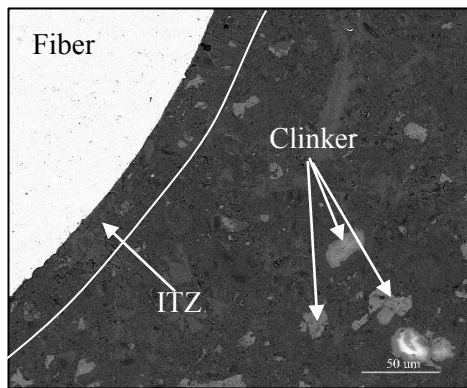


Figure 5. SEM detail of ITZ

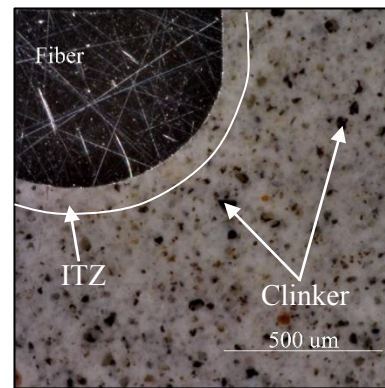


Figure 6. Light microscopy image of ITZ

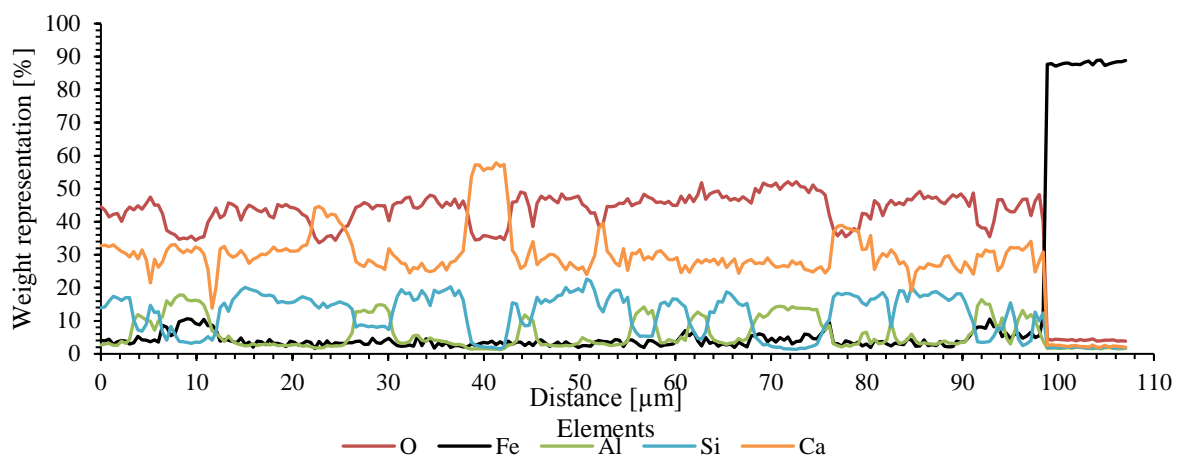


Figure 7. Relative weight ratios by 5 main elements on an EDS linescan

4. Micromechanical performance of ITZ around fiber

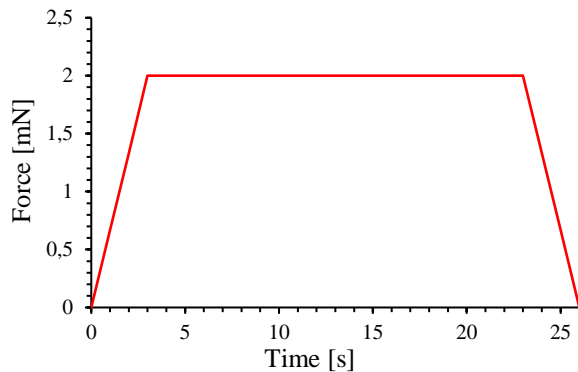
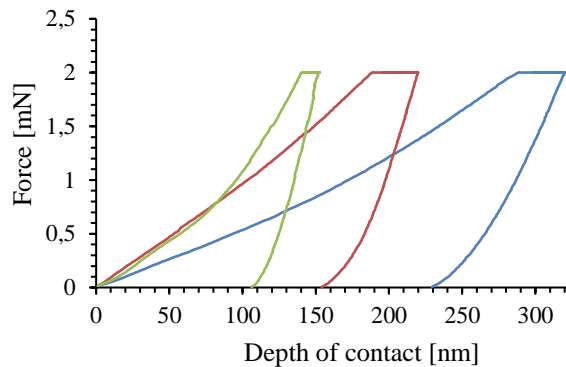
4.1. Nanoindentation parameters

As previously mentioned, the tested sample was prepared by saw cutting, grinding and polishing procedure prior to testing. Since roughness has direct influence to the quality of the measurement, it was checked before the experiment and kept within acceptable level which is in tens of nm.

Two positions on the sample were tested. First, a series of indents in the bulk matrix was conducted. Second, a series of indents in ITZ around the fiber was performed.

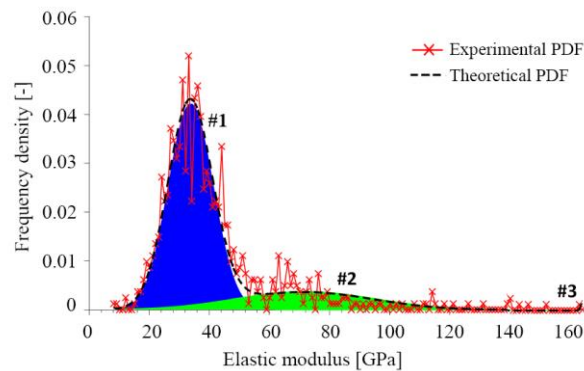
Nanohardness tester Hysitron TriboLab TI-700 equipped with Berkovich diamond tip was used. Load controlled test lasting for 26 seconds was prescribed to the maximum force of 2000 μN for each indent. The load function had a trapezoidal shape (Fig. 8). The first part of the function was a linear loading with speed of 40 mN/min lasting for 3 seconds. The second part was a constant loading for 20 seconds and the last part of the function was a linear unloading for 3 seconds.

A typical response (load-depth record) for various phases in the material is shown in Fig. 9. The material properties were evaluated for each indent by the Oliver and Pharr [15] method. Subsequently, discrimination between the phases was done by statistical deconvolution in the bulk measurements [1,14].

**Figure 8.** Load of function of indents**Figure 9.** Indentation curves

4.2. Micromechanical response of the bulk cement paste

The results of the bulk cement paste were taken from authors' previous work [1] and is summarized here for readers convenience. The sample surface was covered with series of matrices with size of $10 \times 10 = 100$ indents with was $12,5 \mu\text{m}$ separation in between the indents. Overall, 850 indents were done. Elastic moduli were calculated by the theory of Oliver and Pharr [15]. Distributions of elastic moduli for individual micromaterial phases were determined using deconvolution method [1,14]. The resulting histogram of phase moduli is depicted in Fig. 10 an summarized in Tab. 2. The phase #1 corresponds to C-S-H gel, CAH and part of CH, #2 to mainly CH and small particle particle leftover of clinkers and #3 to large clinkers [1]. Note, that the number and volume fractions of the mechanical phases (Tab. 2) do not match exactly the chemically different phases found in the image analysis (Tab.1) although there is a certain overlap.

**Figure 10.** Histogram of theoretical and experimental probability density of elastic modulus in cement paste**Table 2.** Values of modulus of elasticity for individual micromechanical phases in cement paste

	#1	#2	#3
Average value E [GPa]	33,58	70,51	164,59
Standard daviation [GPa]	7,3	22,83	0,55
Volume ratio [%]	77,72	22,03	0,25

4.3. Nanoindentation in ITZ

A series of indents was done in the ITZ around steel fiber in cement paste. Several rows leading in perpendicular direction to the fiber were performed. The separation of indents was lowered to 2 to $4 \mu\text{m}$.

The Hysitron-700 system allows to make in-situ scan prior the indentation. The surface scan (similar to AFM scan) is shown in Fig. 11. The scan allows also precision positioning of the indents in

the wanted direction. A row of prescribed 17 indents and resulting imprints scanned afterwards is depicted in Fig. 11.

The first two indents were prescribed on the surface of the steel fiber and other indents were positioned in ITZ and later in the bulk material coming from the fiber to the cement matrix. Some defective indentations caused by local porosity or roughness were eliminated from considerations. Overall, 27 rows in 10 regions around the steel fiber was done. In total, 336 indents were used for evaluation. The same methodology used for the bulk was also used here, i.e. the Oliver and Pharr [15] was used for obtaining modulus of elasticity for a single indent and profiles of the property were constructed for each row.

An example of individual row measurements is shown in Fig. 11 and 12 where microstructural position of rows and corresponding elastic moduli are shown.

Figure 13 shows average modulus of elasticity calculated from merged results from all respective positions with standard deviations. The graph shows a general trend of decreasing modulus as the position is closer to the fiber. A linear trend line was calculated and indicated in Fig. 13 which also shows an average bulk elastic modulus obtained from homogenization (calculated later in the paper) to which the ITZ modulus approaches.

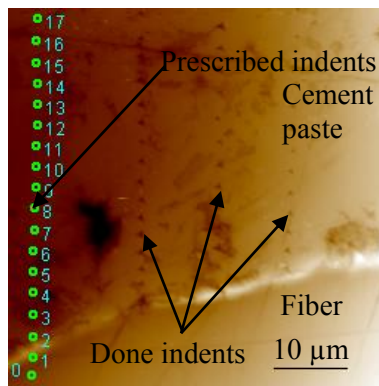


Figure 11. Scan of investigated region with marked and indented rows

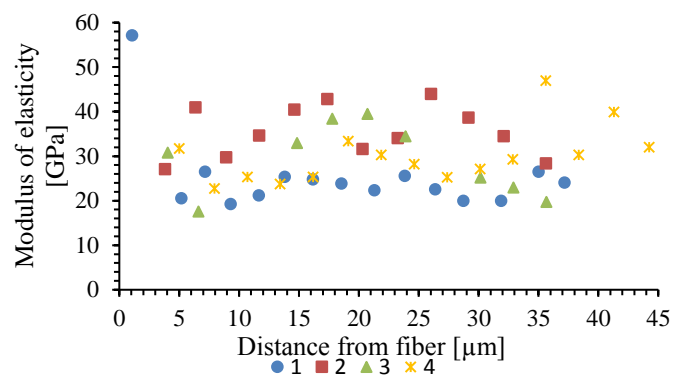


Figure 12. Profile of elastic moduli at individual positions (each colour indicates a group of indents belonging to a row)

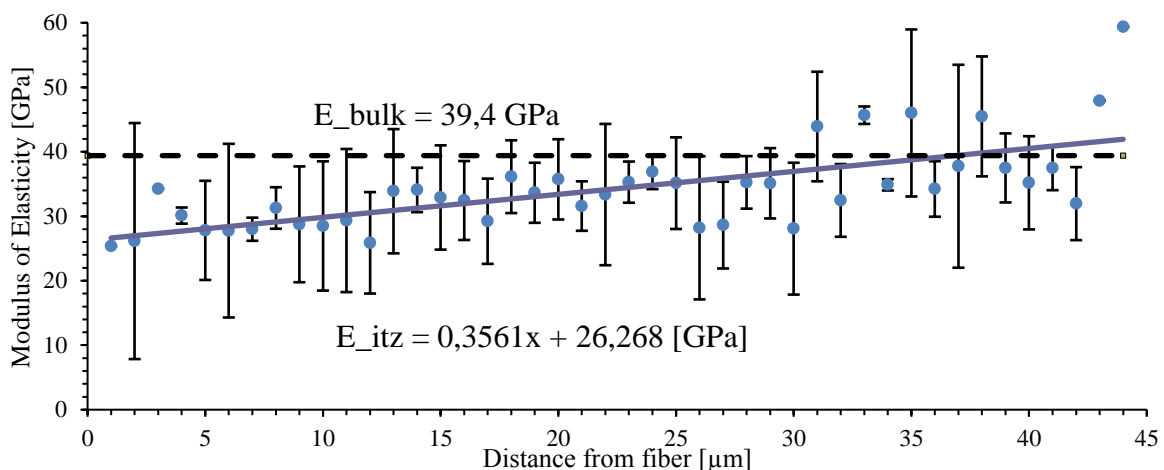


Figure 13. The dependence of an average elastic modulus on the distance from fiber and its trendline

5. A two-scale model for elastic modulus of fiber reinforced composite with ITZ

A simple two-scale model was created for demonstration of the influence ITZ on the overall elastic behaviour of the steel fiber reinforced cement paste. The first (lower) level of the model is composed of cement paste that further consists of four micromechanical phases obtained from nanoindentation

(Tab. 2). The second (upper) level is assumed to be composed of homogenized cement paste as matrix phase.

The study provided in this paper is focused on the mechanical influence considering the ITZ presence. Thus, simplified assumptions on the other parameters are therefore taken such as perfect bond of the phases and spherical shape of the inclusions. Other parameters like elastic moduli, volume fractions are taken from direct measurements (nanoindentation).

5.1. Mori Tanaka elastic homogenization

The Mori-Tanaka homogenization scheme assumes inclusions to be dispersed in a homogeneous matrix. The effective stiffness tensor L^{eff} is obtained as

$$L^{eff} = L^{(0)} + \sum_{r=1}^n c^{(r)} (L^{(r)} - L^{(0)}) A^{(r)} (c^{(0)} I + \sum_{r=1}^n c^{(r)} A^{(r)})^{-1} \quad (1)$$

where $L^{(0)}$ is the matrix stiffness tensor, $L^{(r)}$ is individual phase stiffness tensor, $c^{(0)}$ is the volume fraction of the matrix, $c^{(r)}$ is the volume fraction of individual phase, I is the fourth order unity tensor and $A^{(r)}$ is the concentration factor determined by Eshelby's inclusion problems solution as

$$A^{(r)} = [I + S M^{(0)} (L^{(r)} - L^{(0)})]^{-1} \quad (2)$$

where $M^{(0)}$ is the matrix compliance tensor and S is the Eshelby tensor which depends only on the geometrical shape of an inclusion and material parameters of the matrix. For spherical inclusions embedded in an isotropic matrix the Eshelby tensor reduces to

$$S = \alpha^{(0)} I_v + \beta^{(0)} I_d \quad (3)$$

where I_v and I_d are volumetric and deviatoric parts of the unity tensor, respectively $\alpha^{(0)}$ and $\beta^{(0)}$ are

$$\alpha^{(0)} = \frac{3K^{(0)}}{3K^{(0)} + 4G^{(0)}}, \quad \beta^{(0)} = \frac{6(K^{(0)} + 2G^{(0)})}{5(3K^{(0)} + 4G^{(0)})} \quad (4)$$

where $K^{(0)}$ is the matrix bulk modulus and $G^{(0)}$ is the matrix shear modulus.

5.2. Results from homogenization

The input parameters for the first level homogenization are listed in Tab. 3. Homogenized elastic modulus obtained with the Mori-Tanaka scheme is 39.40 GPa. This value is sent to the second level homogenization as an input value for the matrix phase there. The second level homogenization input and output parameters are summarized in Tab. 4. A common steel fiber to matrix ratio of 1.5% is used for the present study. The assumption of a bilinear shape of the elastic modulus around fibers is taken (Fig. 13). Minimum elastic modulus estimated in ITZ (26.27 GPa) is considered as the ITZ modulus which is about 67% of the bulk E value. The width of ITZ is assumed to be defined by the point of intersection of the ITZ trend line and the bulk matrix elastic modulus. From Fig. 13, the width is assessed as 37 μ m. Due to the uncertainty in the ITZ width estimate, a parametric study considering three ITZ widths (20, 40 and 60 μ m) is performed. The volumetric content of the ITZ phase in a composite is given by the fiber dimensions and the ITZ width (for a single fiber the ITZ volume is given by the fiber surface area (165 mm²) times the ITZ width 0.037 mm and is equal to 6.1 mm³).

Negligible differences have been found for varying ITZ width in the given range and the homogenized composite elastic modulus was calculated as \sim 40.2 GPa (Tab. 4).

Table 3. Level 1- cement paste level homogenization

Phase	Vol. fraction	E [GPa]
#1 (matrix phase)	0.7772	33.58
#2	0.2203	70.51
#3	0.0025	164.59
Level 1-homogenized E (GPa)	1	39.40

Table 4. Level 2 - composite level homogenization

Phase	Vol. fraction	E [GPa]
Level 1 (matrix)	0.9829	39.40
Fibers	0.015	200
0. no ITZ, or	0	-
a. ITZ 20 μm , or	0.0011	26.27
b. ITZ 40 μm , or	0.0023	26.27
c. ITZ 60 μm	0.0034	26.27
Level 2-homogenized, case 0	1	40.25
Level 2-homogenized, case a	1	40.23
Level 2-homogenized, case b	1	40.21
Level 2-homogenized, case c	1	40.19

6. Discussion

Clearly, the ITZ width does not have a significant influence on the composite elastic modulus due to its negligible volumetric content in the mixture. This conclusion can be partially influenced by simplified assumptions (mainly the perfect bonding of the phases and spherical shape of inclusions). However, no major influence on the elastic modulus can be anticipated and the composite modulus does not vary much with or without considering ITZ in the homogenization. The reason is that the homogenized property depends mainly on the volumetric content of individual phases. In other words, volumetrically small phases have small influence on the resulting elastic modulus. Thus, neither small volumetric content of fibers (1.5%) nor ITZ content (0.1-0.3%) changes the cement paste elastic modulus much (pure cement paste $E=39.40$ GPa and composite $E=40.2$ GPa).

However, about 67% decrease in elastic modulus with respect to the cement bulk indicates also lower strength that is known to have the same trend as elastic modulus in concrete. It can be anticipated that the strength of a composite will be dictated by the weakest phase in the composite rather than its volumetric content. In this sense, the decreased ITZ properties and an approximate size of ITZ found in this paper can serve as input parameters to a fracture based model. Thus, future work should concentrate on the assessment of strength and fracture properties of ITZ and bulk and development of the composite strength model. Such model is, however, beyond the scope of the present paper.

7. Conclusion

The presented paper provides a micromechanical, microstructure and chemical study on ITZ between steel fiber and cement matrix. Microstructure of ITZ around fibers is characterized with less portion of clinkers than in a bulk matrix. Nanoindentation was used to deliver microscale elastic properties. An average modulus of elasticity of ITZ calculated from merged nanoindentation results showed a general trend of decreasing modulus as the position was closer to the fiber. A Minimum elastic modulus estimated in the ITZ (26.27 GPa) was considered as the ITZ modulus that is about 67% of the bulk E value. Homogenized elastic modulus of the bulk material obtained by the Mori-Tanaka scheme was calculated as 39.4 GPa. Taking fibers and ITZ into account, the second level homogenization exhibited composite elastic modulus of 40.2 GPa. The ITZ width does not have a significant influence on the composite modulus due to its negligible volumetric content in the mixture (0.1-0.3%).

However, it can be anticipated that the strength of composite will be defined by the weakest phase strength in the composite (which was proved to be ITZ) rather than its volumetric content.

Acknowledgement

Financial support of the Czech Science Foundation (project 17-05360S) is gratefully acknowledged. L. Polívka (Academy of Sciences, CZ) is acknowledged for his help with acquisition of SEM images.

References

- [1] Němeček, J. *Mikromechanické vlastnosti cementových kompozitů*, Diplomová práce, Praha: ČVUT, Fakulta Stavební, 01/2017
- [2] Němeček, J., Králík, V., Šmilauer, V., Polívka, L., Jäger, A. *Tensile strength of hydrated cement paste phases assessed by micro-bending tests and nanoindentation*, Cement and Concrete Composites 73 (2016), pp 164-173
- [3] Diamond, S., Huang, J. *The ITZ in concrete – a different view based on image analysis and SEM observations*, Cement and Concrete Composites 23 (2001), pp 179-188
- [4] Petráňová, V., Sajdllová, T., Němeček, J. *Micromechanical Homogenization of Ultra-High Performance Concrete*, Applied Mechanics and Materials Vol. 821 (2016), pp 518-525
- [5] Nežerka, V., Němeček, J., Sližkova, Z., Tesárek, P. *Investigation of crushed brick-matrix interface in lime-based ancient mortar by microscopy and nanoindentation*, Cement & Concrete Composites 55 (2015), pp 122–128
- [6] Scrivener, K. L., Crumbie, A. K., Laugesen, P. *The Interfacial Transition Zone (ITZ) Between Cement Paste and Aggregate in Concrete*, INTERFACE SCIENCE 12 (2004), pp 411–421
- [7] Vargas, P., Restrepo-Baena, O., Tobón, J. I. *Microstructural analysis of interfacial transition zone (ITZ) and its impact on the compressive strength of lightweight concretes*, Construction and Building Materials 137 (2017), pp 381–389
- [8] Allison, P.G., Moser, R.D., Weiss Jr., C.A., P.G. Malone, P.G., Morefield, S.W. *Nanomechanical and chemical characterization of the interface between concrete, glass–ceramic bonding enamel and reinforcing steel*, Construction and Building Materials 37 (2012), pp 638–644
- [9] Zhu, W., Bartos, P.J.M. *Application of depth-sensing microindentation testing to study of interfacial transition zone in reinforced concrete*, Cement and Concrete Research 30 (2000), pp 1299-1304
- [10] Wang, X. H., Jacobsen, S. He, J. Y., Zhang, Z. L., Lee, S. F., Lein, H. L. *Application of nanoindentation testing to study of the interfacial transition zone in steel fiber reinforced mortar*, Cement and Concrete Research 39 (2009), pp 701–715
- [11] Hashin, Z., Monteiro, P.J.M. *An inverse method to determine the elastic properties of the interphase between the aggregate and the cement paste*, Cement and Concrete Research 32 (2002), pp 1291–1300
- [12] Zhang J., Sun H., Wan J., Yi Z., *Study on microstructure and mechanical property of interfacial transition zone between limestone aggregate and Sialite paste*, Construction and Building Materials 23 (2009), pp 3393–3397
- [13] Acker, P. *Swelling, shrinkage and creep: a mechanical approach to cement hydration* Material Structure, 37 (4) (2004), pp 237–243
- [14] Němeček, J., Kralík, V., Vondřejc, J. *Micromechanical analysis of heterogeneous structural materials*, Cement & Concrete Composites 36 (2013), pp 85–92
- [15] Oliver, W.C., Pharr, G.M. *An improved technique for determining hardness and elastic modulus using load and displacement sensing indentation experiments*, Journal of Material Research 7 (1992), pp 1564-1583